

ANALYSIS OF EXTREME-ULTRAVIOLET SPECTROHELIOGRAMS OF SOLAR PROMINENCES

MITSUO KANNO*, GEORGE L. WITHBROE, and ROBERT W. NOYES

Harvard-Smithsonian Center for Astrophysics, 60 Garden Street, Cambridge, MA 02138, U.S.A.

(Received 24 January; in revised form 20 June, 1980)

Abstract. The optical depth at the head of the Lyman continuum, τ_{H} , is determined at a number of positions in three hedgerow prominences using spectroheliograms ($5'' \times 5''$ resolution) of C III $\lambda 977$, LC $\lambda 896$, and O IV $\lambda 554$ observed with the Harvard experiment on Skylab. At heights greater than $10''$ above the limb the maximum value of τ_{H} is 30 to 50, which occurs at the central part of the prominences. For one of the prominences the determination of τ_{H} is found to be consistent with data from spectroheliograms of Mg $\times \lambda 625$. The degree of ionization of hydrogen is estimated from the intensity of LC $\lambda 896$ at $\tau_{\text{H}} \gg 1$. In the central part of a model prominence $N_{\text{p}}/N_{\text{HI}} \leq 1.9$ for a reasonable range of the electron densities, where N_{p} and N_{HI} are the proton density and the neutral hydrogen density, respectively.

1. Introduction

During the Skylab mission a large number of prominences of all types were observed in wavelengths ranging from the X-ray to visual regions of the spectrum. Extreme-ultraviolet (EUV) measurements from the Harvard experiment have been reported by Schmahl *et al.* (1974) and Orrall and Schmahl (1976). Feldman and Doschek (1977) and Kjeldseth Moe *et al.* (1979) reported EUV observations obtained with the Naval Research Laboratory experiment.

A major problem in the physics of prominences is the derivation of the opacity in the Lyman continuum (LC) and the degree of ionization of hydrogen. Most studies of this problem have been made either by an indirect method using empirical data in the visual spectrum or by theoretical calculations assuming a simplified model of the prominence (e.g., Tandberg-Hanssen, 1974; Hirayama, 1979). The purpose of this analysis is an empirical determination of these parameters from EUV spectroheliograms of prominences.

The observations used in this investigation were acquired by the Harvard College Observatory's ATM experiment (S055) on Skylab (Reeves *et al.*, 1974, 1977a). The instrument was capable of producing spectroheliograms of $5' \times 5'$ region in 5.5 min with a spatial resolution of $5'' \times 5''$. Data could be obtained simultaneously at up to seven wavelengths between 280 and 1350 Å. For the analysis we utilized spectroheliograms of C III $\lambda 977$, LC $\lambda 896$, Mg $\times \lambda 625$, and O IV $\lambda 554$ which were obtained at the primary polychromatic setting of the instrument.

2. Optical Depth in the Lyman Continuum

The optical depth at the Lyman limit, τ_{H} , of prominences was earlier found to be ≈ 100 from observations of singly ionized metal lines in the visual wavelength range

* Present address: Hida Observatory, University of Kyoto, Kamitakara-mura, Gifu-ken 506-13, Japan.

(Hirayama, 1963, 1964). These results may be affected by uncertainties in the abundance ratios, the excitation conditions, etc. The values of τ_H can be more directly deduced from the LC attenuation effect in EUV transition-region lines of prominences. Using this method Orrall and Schmahl (1976) found $\tau_H \leq 10$ in most of the prominences studied. Their analysis is based on measurements of the ratio of the intensity of a line measured at the center of the quiet Sun within a supergranule cell to its intensity in the prominence. Their results should be corrected for the LC attenuation effect in EUV lines at the disk center itself which has been found by Kanno (1979) and Schmahl and Orrall (1979). This would increase the values for the optical depths found by Orrall and Schmahl. On the other hand, a wide range of τ_H was found from recent theoretical models of prominences which fit observed constraints (Heasley and Mihalas, 1976; Heasley and Milkey, 1976, 1978). In the following, EUV spectroheliograms will be used to deduce the two-dimensional distribution of τ_H in prominences.

2.1. METHOD

Simultaneous spectroheliograms of C III $\lambda 977$, LC $\lambda 896$, and O IV $\lambda 554$ may be used to determine τ_H from the LC attenuation effect in O IV $\lambda 554$. We assume a multiple-slab model for the prominence introduced by Orrall and Schmahl (1976). In this model the prominence is viewed as consisting of a number of cool ($T < 10^4$ K) and identical slabs embedded in the hot ($T \approx 10^6$ K) corona; at the surface of each slab is a transition zone of intermediate temperature. The observed intensity of C III $\lambda 977$ and O IV $\lambda 554$ will be

$$I(\text{C III}) = 2NI_{\text{C III}}, \quad (1)$$

and

$$I(\text{O IV}) = I_{\text{O IV}} \left[1 - e^{-N\tau_1} + 2 \sum_{n=1}^N e^{-n\tau_1} \right]. \quad (2)$$

Here $I_{\text{C III}}$ and $I_{\text{O IV}}$ are the intensity of C III $\lambda 977$ and O IV $\lambda 554$ emitted by the transition zone at each surface of the slabs, N is the number of the slabs in the line of sight, and τ_1 is the optical depth of one slab in the LC at $\lambda_1 = 554 \text{ \AA}$. In Equations (1) and (2) we have assumed that C III $\lambda 977$ and O IV $\lambda 554$ are optically thin. We shall discuss self-absorption effects of these lines in Section 2.2.

From Equations (1) and (2) we have

$$R \equiv \frac{I(\text{C III})}{I(\text{O IV})} = \frac{I_{\text{C III}}}{I_{\text{O IV}}} \alpha^{-1}, \quad (3)$$

where α is the LC attenuation factor defined by Orrall and Schmahl (1976):

$$\alpha = \frac{1 - e^{-N\tau_1} + 2 \sum_{n=1}^N e^{-n\tau_1}}{2N}. \quad (4)$$

We now assume that the total optical depth $N\tau_1$ is finite, but that the number of individual slabs is very large; i.e. the hot and cold regions of the prominence are intimately mixed. In the limit where N approaches infinity (and τ_1 approaches zero), α approaches the limit

$$\lim_{N \rightarrow \infty} \alpha = \frac{1 - e^{-\tau_t}}{\tau_t}, \quad (5)$$

where τ_t is the total optical depth of the slabs in the LC at 554 Å. In the following we use the limit instead of α , so that we have

$$R = \frac{I_{CIII}}{I_{OIV}} \frac{\tau_H(\lambda_1/\lambda_H)^3}{1 - e^{-\tau_H(\lambda_1/\lambda_H)^3}}, \quad (6)$$

where λ_H is the wavelength at the head of the LC: $\lambda_H = 912$ Å. We note that the assumption $N \rightarrow \infty$ gives a lower limit for the optical depth (see Orrall and Schmahl, 1976, Figure 3). If the number of threads is greater than 10, then the maximum error in τ_H is only 10%.

Now we can determine τ_H from Equation (6) using the observed intensity ratio R , provided that the ratio I_{CIII}/I_{OIV} is known. The ratio I_{CIII}/I_{OIV} may in principle be calculated if one knows the structure of the transition region between the prominence and the corona. However, the calculated value of I_{CIII}/I_{OIV} may contain uncertainties introduced by imprecise knowledge of the atmospheric structure as well as uncertainties in the abundance ratio, the atomic data, the excitation conditions, etc. Furthermore, there may be a possibility that the value of I_{CIII}/I_{OIV} differs among the prominences. Nevertheless, with the aid of the observed intensity of LC $\lambda 896$, we are able to deduce empirically the relation between τ_H and R and thus indirectly determine I_{CIII}/I_{OIV} from Equation (6). We describe this procedure below.

Assuming the source function of the LC to be constant with depth and position in a prominence, we have the intensity of the LC at $\lambda 896$,

$$I(\text{LC}) = S_{\lambda_c} [1 - e^{-\tau_H(\lambda_c/\lambda_H)^3}], \quad (7)$$

where S_{λ_c} is the source function of the LC at $\lambda_c = 896$ Å. The assumption of a constant S_{λ_c} will be discussed in Sections 2.2 and 2.3. From Equations (6) and (7) we have

$$\frac{d[\log I(\text{LC})]}{d[\log R]} = \frac{\tau_H(\lambda_c/\lambda_H)^3}{e^{\tau_H(\lambda_c/\lambda_H)^3} - 1} \frac{e^{\tau_H(\lambda_1/\lambda_H)^3} - 1}{e^{\tau_H(\lambda_1/\lambda_H)^3} - 1 - \tau_H(\lambda_1/\lambda_H)^3}. \quad (8)$$

The gradient $d[\log I(\text{LC})]/d[\log R]$ is independent of I_{CIII}/I_{OIV} and S_{λ_c} . For large τ_H (or R) the gradient has a value ≈ 0 ; it reaches a value of unity at $\tau_H = 2.46$ and then rapidly increases with decreasing τ_H (or R) for $\tau_H < 2.46$. The value of R at which the gradient becomes unity (R_1) will be found from a diagram of $\log I(\text{LC})$ vs $\log R$ plotted for a number of positions in a prominence. Assuming the value of I_{CIII}/I_{OIV}

to be constant in a single prominence, then we can find the numerical relation between τ_H and R , that is, the value of $I_{C\text{ III}}/I_{O\text{ IV}}$ for the prominence.

2.2. RESULTS

For this analysis we selected three hedgerow prominences (see Table I) from those studied by Orrall and Schmahl (1976). The measurements of spectroheliograms were converted into the absolute intensity based on the photometric calibration of the Harvard spectrometer by Reeves *et al.* (1977b). The outer boundary of the prominence was defined as the contour of the intensity of C III λ 977 with a value of 10% of the mean prominence intensity. This boundary coincides well with that observed in the *La* image of the prominence. The location of the limb was determined by extrapolation of the limb contour of O IV λ 554 outside the prominence.

TABLE I
Data of the prominences

Prominence	UT date and time of limb observations	Heliocentric position of prominence ^a		
		Long. (Carr. rot.)	Lat.	P.A.
P23	1973 Aug. 08, 00:41	280° (1604)	10° N	280°
P28A	1973 Aug. 16, 18:11	160° (1604)	35° N	305°
P42	1973 Aug. 30, 21:23	320° (1605)	28° S	242°

^a From the data given by Orrall and Schmahl (1976).

Figure 1 displays $I(\text{LC})$ in units of $\text{erg cm}^{-2} \text{s}^{-1} \text{sr}^{-1} \text{\AA}^{-1}$ as a function of R on a logarithmic scale for the three prominences. The background intensity, which is usually less than $1 \text{ erg cm}^{-2} \text{s}^{-1} \text{sr}^{-1} \text{\AA}^{-1}$, has not been subtracted from $I(\text{LC})$. The points in Figure 1 are restricted to heights greater than $10''$ above the limb in order to avoid effects of chromospheric structures such as spicules, fibrils, and network walls along the line of sight. Also, two positions of P28A are disregarded where the chromospheric material seems to protrude into the line of sight. Several points for P28A and P42 with $I(\text{LC}) < 1 \text{ erg cm}^{-2} \text{s}^{-1} \text{sr}^{-1} \text{\AA}^{-1}$ are excluded from Figure 1.

Figure 1 shows that $I(\text{LC})$ is constant for large R (or large τ_H) within a factor of 2 except for a few points which occur near the outer boundary and at a particular portion of the prominences. Most of the points with large R in Figure 1 correspond to the central part of the prominences. Therefore, the assumption of a constant S_{λ_c} in Equation (7) is consistent with the observations at least in the central part of the prominences.

Figure 1 shows that $I(\text{LC})$ decreases with decreasing R below some value of R . This seems to be caused by decreasing opacity in the LC according to Equation (7). However, there could be an alternative possibility – that the decrease of $I(\text{LC})$ reflects a decrease in the slit-filling factor, f_s , which is the fraction of the prominence

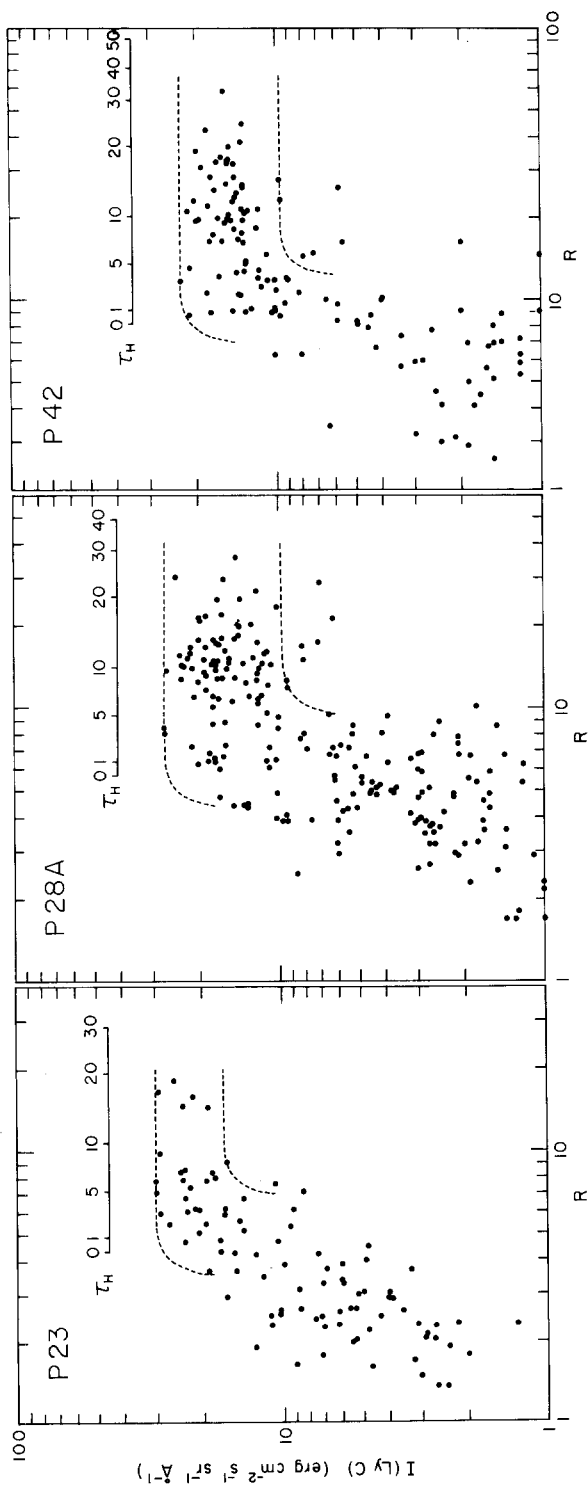


Fig. 1. Intensities of the LC at 896 Å as a function of R for three prominences. Dashed lines calculated from Equations (6) and (7) are drawn at possible positions corresponding to the outer and inner envelopes of the points for each prominence. The scale of τ_H is based on the adopted value of $I_{\text{CIV}}/I_{\text{OIV}}$ for each prominence. Several points with $I(\text{LC}) < 1 \text{ erg cm}^{-2} \text{ s}^{-1} \text{ sr}^{-1} \text{ \AA}^{-1}$ are excluded for P28A and P42.

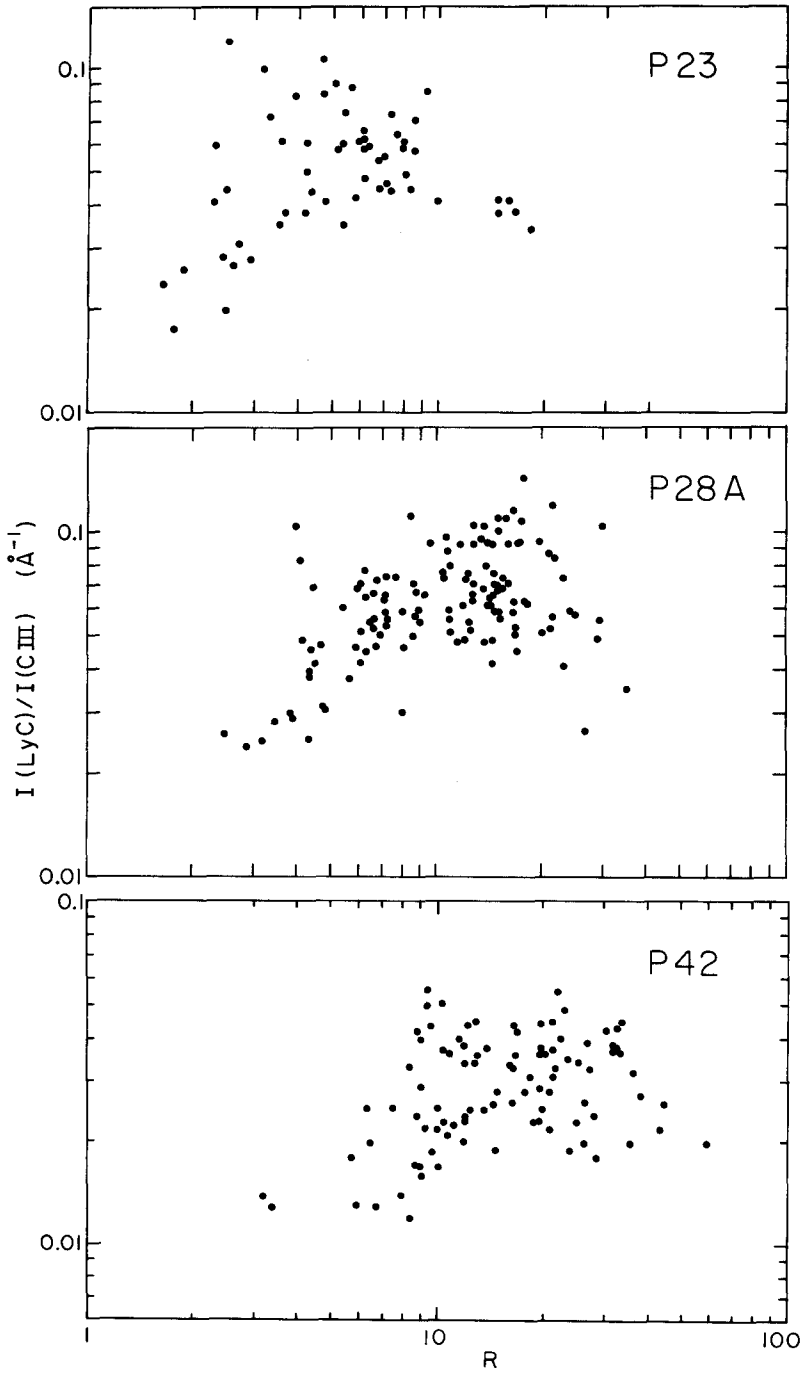


Fig. 2. LC $\lambda 896/\text{C III } \lambda 977$ ratios as a function of R . The points are restricted to positions in the prominences where $I(\text{LC})$ is greater than 7, 5, and 3 $\text{erg cm}^{-2} \text{s}^{-1} \text{sr}^{-1} \text{\AA}^{-1}$ for P23, P28A, and P42, respectively.

threads filling the $5'' \times 5''$ slit. We discuss (and rule out) this alternative possibility below.

In order to investigate the effect of f_s , we have plotted the ratio $I(\text{LC})/I(\text{C III})$ as a function of R in Figure 2. The points in Figure 2 are restricted to positions in the prominences where $I(\text{LC})$ is greater than 7, 5, and 3 $\text{erg cm}^{-2} \text{s}^{-1} \text{sr}^{-1} \text{\AA}^{-1}$ for P23, P28A, and P42, respectively. This is necessary to avoid contamination due to the background intensity of the LC around the prominences resulting from scattering of chromospheric radiation by the optics of the telescope. If the decrease of $I(\text{LC})$ in Figure 1 were due to a decrease in f_s , $I(\text{LC})/I(\text{C III})$ would be more or less constant with R , because the thickness of the transition region of the prominence threads is very small (Schmahl *et al.*, 1974). However, Figure 2 indicates that $I(\text{LC})/I(\text{C III})$ also tends to decrease with decreasing R below some value of R . Thus we conclude that the decrease of $I(\text{LC})$ in Figure 1 comes mainly from the opacity effect of the LC.

In Figure 1 we have illustrated theoretical curves (dashed lines) derived from Equations (6) and (7), but choosing the parameters $I_{\text{C III}}/I_{\text{O IV}}$ and $S_{\lambda c}$ arbitrarily, so as to place the curves at locations corresponding to the outer and inner envelopes of the points for each prominence. From these curves we found a possible range of R_1 (the value of R where $d[\log I(\text{LC})]/d[\log R] = 1$) for each prominence which is listed in Table II along with the geometric mean, $\langle R_1 \rangle$. Given that $\langle R_1 \rangle$ corresponds to $\tau_{\text{H}} = 2.46$, as indicated earlier, we can derive $I_{\text{C III}}/I_{\text{O IV}}$ for each prominence. These values for $I_{\text{C III}}/I_{\text{O IV}}$ (which are given in Table II) can then be used with Equation (6) to calculate τ_{H} as a function of R . The latter relationships are given in Figure 1.

TABLE II
Results of the analysis

Prominence	R_1	$\langle R_1 \rangle$	$\frac{I_{\text{C III}}}{I_{\text{O IV}}}$	$I(\text{LC})^a$	b_1	
				($\text{erg cm}^{-2} \text{s}^{-1} \text{sr}^{-1} \text{\AA}^{-1}$)	6600 K	6800 K
P23	4-8	5.6	4.3	24.1 (± 3.9)	2.3	4.7
P28A	5-11	7.4	5.7	16.5 (± 3.9)	3.4	6.9
P24	8-14	10.6	8.1	15.3 (± 2.8)	3.6	7.4

^a The average of $I(\text{LC})$ at positions with $\tau_{\text{H}} \geq 10$. The number in the parentheses is the standard deviation.

It is interesting that the three prominences have different values of $I_{\text{C III}}/I_{\text{O IV}}$. This can also be inferred from Figure 2 in which $I(\text{LC})/I(\text{C III})$ begins to decrease with decreasing R at different values of R for the three prominences. This fact may be caused by differences in the structure of the transition region of the prominence threads and of the region between the threads.

Figure 1 shows a number of points which have values of R less than the lower limit $R_{\text{min}} = I_{\text{C III}}/I_{\text{O IV}}$ predicted by this simple model. Thus, rather than falling between the two asymptotic values of R indicated by the dashed lines, the points in Figure 1

with smallest $I(\text{LC})$ also have smaller values of R , and follow the approximate relation $d[\log I(\text{LC})]/d[\log R] \approx 2$. The points in question also lie near the edges of the prominences, rather than near their centers. We interpret this finding as due to the fact that in locations near the edge of the prominence the fill factor f_s for the Lyman-continuum-emitting threads and their transition zones is considerably less than unity. If we postulate the existence of hot ($T > 10^{5.5}$ K) material between the threads in line with the findings of Orrall and Schmahl (1976), see their Figure 2), then this material would emit negligible C III ($\log T_{\max} = 4.95$) compared to O IV ($\log T_{\max} = 5.25$). The slope $d[\log I(\text{LC})]/d[\log R] \approx 2$ would be explained if, in the region of Figure 1 considered (i.e. $R/R_{\min} \approx \frac{1}{2}$), the O IV emission from the regions between the threads was comparable to that of the transition regions around the threads, while the C III emission from the region between the threads was negligible compared to that of the threads. In determining τ_H we assumed that positions with $R < R_{\min}$ are optically thin in the LC ($\tau_H < 1$).

We have so far neglected self-absorption effects of C III $\lambda 977$ and O IV $\lambda 554$. Schmahl *et al.* (1974) found that all the transition-region lines of the prominence longward of the Lyman limit are optically thin with the exception of C III $\lambda 977$. They inferred that the optical depth in C III $\lambda 977$ averaged over the line profile is $\tau(\text{C III}) = 0.33 \pm 0.05$ in the prominence just above the limb. This is comparable with $\tau(\text{C III})$ at the disk center of the quiet Sun (see Withbroe, 1970). On the other hand, the optical depth of the prominence in O IV $\lambda 554$ may be negligible, because $\tau(\text{O IV})$ at the disk center of the quiet Sun is very small (Withbroe, 1970). Therefore, the observed ratio R in the central part of the prominences should be corrected for the self-absorption effect of C III $\lambda 977$ with $\tau(\text{C III}) \approx 0.33$. This correction results in an increase in R of about 40%.

Making the correction for the self-absorption effect of C III $\lambda 977$, we conclude from Figure 1 that the maximum value that τ_H attains is 30 to 50 in the central part of the three prominences at heights greater than $10''$ above the limb. At $\tau_H = 50$, the LC attenuation factor α for O IV $\lambda 554$ is ≈ 0.09 . This means that the number of the prominence threads along the line of sight should be larger than five on the assumption of the multiple-slab model (see Figure 3, Orrall and Schmahl, 1976).

Figure 3 shows the two-dimensional distribution of τ_H for the three prominences above the limb. A square in Figure 3 represents an area $5'' \times 5''$ ($\approx 3650 \times 3650 \text{ km}^2$). In Figure 3 no correction has been made for the self-absorption effect of C III $\lambda 977$. The value of τ_H shown in Figure 3 should not be affected very much by a decrease in f_s from unity except for positions with low R , because τ_H is determined from the intensity ratio of C III $\lambda 977$ to O IV $\lambda 554$. It is found from Figure 3 that (1) the value of τ_H varies over a wide range from point to point even in a single prominence, (2) the central part of the prominences shows larger values of τ_H , (3) in general, τ_H decreases with height, and (4) τ_H is less than unity at most positions near the outer boundary of the prominences. A rapid decrease of τ_H with height may be explained if $N_p N_c / N_1 \approx$ constant, which is expected for radiative ionization.

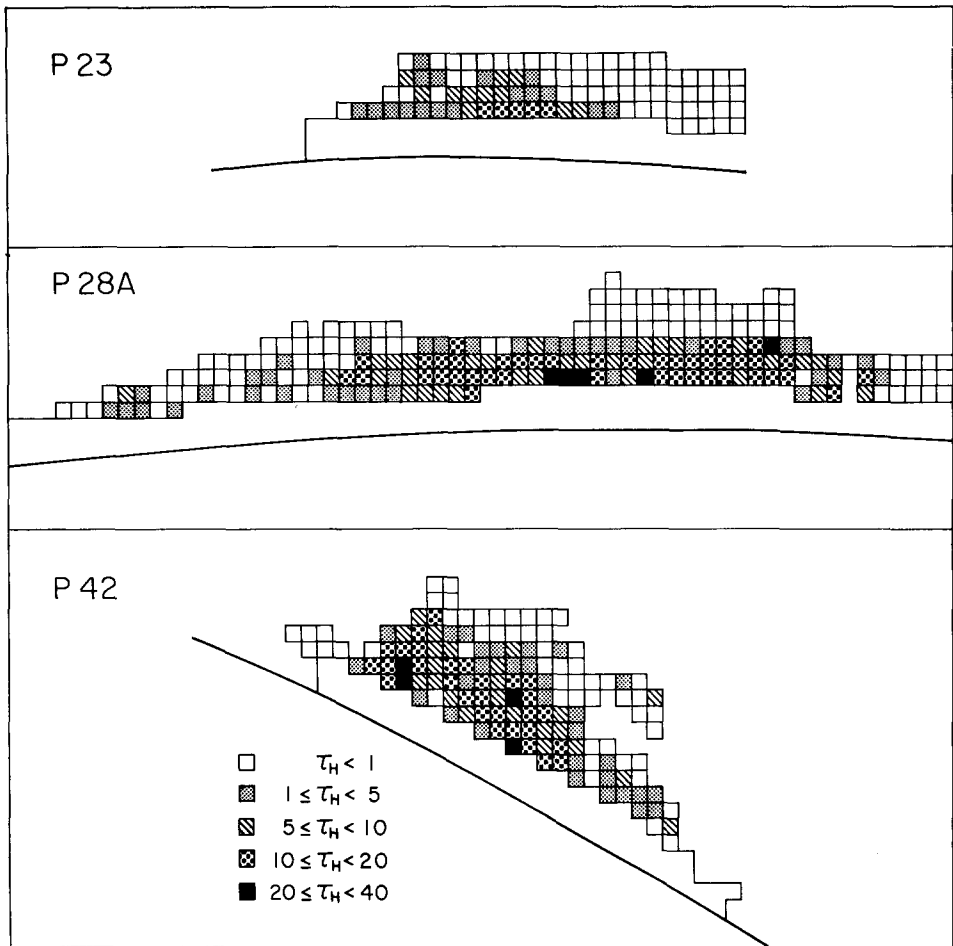


Fig. 3. Two-dimensional distribution of τ_H at heights greater than $10''$ above the limb. A square corresponds to an area of $5'' \times 5''$ ($\approx 3650 \times 3650 \text{ km}^2$). No correction is made for the self-absorption effect of C III $\lambda 977$ (see text).

2.3. COMPARISON WITH THE Mg X SPECTROHELIOGRAM

The prominence, as seen in Mg X $\lambda 625$, is dark due to absorption in the LC of the prominence material (Noyes *et al.*, 1972; Schmahl *et al.*, 1974). The validity of τ_H determined in Section 2.2 may be examined using the data from spectroheliograms of Mg X $\lambda 625$.

The intensity of Mg X $\lambda 625$ observed in the prominence above the limb can be expressed by

$$I(\text{Mg X}) = I_F + I_B e^{-\tau_H (\lambda_2 / \lambda_H)^3}, \tag{9}$$

where I_F and I_B are the Mg X intensity contributing from in front and behind the prominence, respectively, and $\lambda_2 = 625 \text{ \AA}$. Here we have neglected the emission of

Mg x from the region between the prominence threads, because its thickness is much smaller than the distance scale for coronal emission such as $Mg\ x \approx \sqrt{2}R_{\odot}H$, where H is the density scale height). From Equation (9) we have

$$\frac{I(\text{Mg } x)}{I_F + I_B} = \frac{1}{1+A} [A + e^{-\tau_H(\lambda_2/\lambda_H)^3}], \quad (10)$$

where $A \equiv I_F/I_B$. In Equation (10) $I_F + I_B$ is the intensity of Mg x $\lambda 625$ from the corona that would be observed if the prominence were not present, so $I(\text{Mg } x)/(I_F + I_B)$ is the darkness of the prominence in Mg x. At positions in the prominence with $\tau_H \gg 1$, we have $I(\text{Mg } x)/(I_F + I_B) \approx A/(1+A)$. Therefore, the darkness in the Mg x image of the prominence depends on whether $A \ll 1$ or $A \gg 1$.

For examining the validity of τ_H determination, we should select a prominence with $A \ll 1$. Meanwhile, we must know $I_F + I_B$ in the prominence by downward extrapolation of $I(\text{Mg } x)$ above the prominence. To obtain a reliable extrapolation, we should select a prominence around which the emission of Mg x is as intense as possible. From these conditions we selected P23 for the comparison with the spectroheliogram of Mg x $\lambda 625$.

In the spectroheliograms of P23 the lines of raster scan are nearly in the radial direction of the Sun. Therefore, we extrapolated $I(\text{Mg } x)$ above the prominence for each line of the raster scan of P23. Figure 4 shows $I(\text{Mg } x)/(I_F + I_B)$ vs R for each position of P23. It is found from Figure 4 that positions with $R < I_{CIII}/I_{OIV}$ ($=4.3$) are optically thin in the LC ($\tau_H < 1$) as has been assumed in Section 2.2. Assuming A

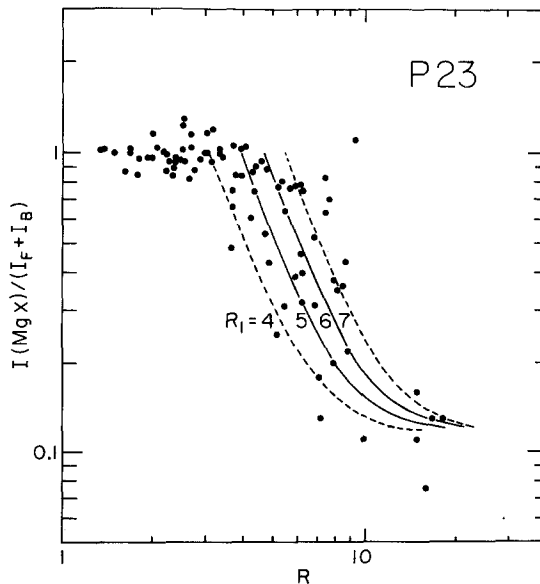


Fig. 4. Ratios of observed to extrapolated intensities of Mg x $\lambda 625$ as a function of R for P23. Curves are calculated from Equations (6) and (10) with $A = 0.14$ for $R_1 = 4, 5, 6, \text{ and } 7$.

to be constant at all positions of P23, we found $A = 0.14$ from the average of $I(\text{Mg } x)/(I_F + I_B)$ for points with $R > 10$ in Figure 4.

The theoretical curves of $I(\text{Mg } x)/(I_F + I_B)$ can be calculated from Equations (6) and (10) with parameters of A and R_1 . Figure 4 shows the curves with $A = 0.14$ for $R_1 = 4, 5, 6,$ and 7 . It is found that the curves for $R_1 = 5$ and 6 are in reasonable agreement with the observations of $\text{Mg } x \lambda 625$. Therefore, we conclude that the determination of τ_H for P23 ($\langle R_1 \rangle = 5.6$) in Section 2.2 is consistent with the data of the $\text{Mg } x$ spectroheliogram.

3. Ionization of Hydrogen

The degree of ionization of hydrogen in quiescent prominences has so far been evaluated from observations of the high Balmer lines (or the visual continuous spectrum) and singly ionized metal lines such as Ca II , Ti II , and Si II . Although the results of the several published analyses do not agree very well within themselves, Tandberg-Hanssen (1974) and Hirayama (1979) concluded that, to a first approximation, the ionization is described by $1 \leq N_p/N_{\text{HI}} \leq 10$. Here N_p and N_{HI} are the proton density and the neutral hydrogen density, respectively. However, Hirayama (1979) remarked that a much lower value of N_p/N_{HI} cannot be excluded. Recent theoretical calculations also show a similar range of N_p/N_{HI} at low densities, $N_{\text{HI}} + N_p \leq 10^{11} \text{ cm}^{-3}$ (Poland *et al.*, 1971; Heasley and Mihalas, 1976; Heasley and Milkey, 1976, 1978).

The data of $I(\text{LC})$ obtained in Section 2.2 may be used to estimate the degree of ionization of hydrogen in the central part of the prominences. For $\tau_H \gg 1$, Equation (7) gives

$$I(\text{LC}) \approx S_{\lambda_c}. \quad (11)$$

The source function S_{λ_c} of the LC is given by

$$S_{\lambda_c} \approx \frac{1}{b_1} \frac{2hc^2}{\lambda_c^5} e^{-(h\nu_c/kT)}, \quad (12)$$

where b_1 is the departure coefficient of the ground level of hydrogen, T is the kinetic temperature, and ν_c is the frequency corresponding to λ_c (Noyes and Kalkofen, 1970; Vernazza and Noyes, 1972).

From the definition of b_1 we have

$$\frac{N_e N_p}{N_1} = \frac{1}{b_1} \frac{(2\pi mkT)^{3/2}}{h^3} e^{-\chi_1/kT}, \quad (13)$$

where N_e is the electron density, N_1 is the population of the ground level of hydrogen, and χ_1 is the ionization potential of hydrogen. From Equations (11), (12), and (13) we have

$$\frac{N_e N_p}{N_{\text{HI}}} \approx \frac{(2\pi mk)^{3/2} \lambda_c^5}{2h^4 c^2} T^{3/2} e^{(h\nu_c - \chi_1)/kT} I(\text{LC}), \quad (14)$$

where we have assumed $N_{\text{HI}} \approx N_1$. The factor $T^{2/3} \exp(h\nu_c - \chi_1)/kT$ in Equation (14) is rather insensitive to T . For a possible range of T , $4500 \leq 8500$ K, in the central part of the quiescent prominences (Hirayama, 1979), the factor ranges within $\pm 30\%$ of its value at a mean temperature, $T = 6600$ K, found by Schmahl *et al.* (1974). Therefore, we can estimate the degree of ionization of hydrogen in the central part of the prominences from Equation (14) without exact knowledge of the temperature.

Table II lists the averages of $I(\text{LC})$ observed at positions with $\tau_{\text{H}} \geq 10$ for the three prominences along with the standard deviation. Some peculiar points below the lower theoretical curves in Figure 1 have been excluded in averaging $I(\text{LC})$ (five points for P28A and one point for P42). The published data for the LC intensity at the disk center of the quiet Sun are 36.2 at 900 Å (Dupree and Reeves, 1971) and 37.9 at 895 Å (Vernazza and Reeves, 1978) in units of $\text{erg cm}^{-2} \text{s}^{-1} \text{sr}^{-1} \text{Å}^{-1}$. Therefore, $I(\text{LC})$ at $\tau_{\text{H}} \gg 1$ for the three prominences observed above the limb is nearly half the quiet-Sun intensity, assuming a slit-filling $f_s \approx 1$ at the central part of the prominence (Schmahl *et al.*, 1974). For reference Table II gives the values of b_1 at $T = 6600$ and 6800 K corresponding to the averages of $I(\text{LC})$ for the three prominences. They are consistent with the results of Noyes *et al.* (1972) and Schmahl *et al.* (1974).

From Equation (14) we calculated the degree of ionization of hydrogen and the total and neutral hydrogen density in the central part of a model prominence with $T = 6600$ K and $I(\text{LC}) = 20 \text{ erg cm}^{-2} \text{s}^{-1} \text{sr}^{-1} \text{Å}^{-1}$. From the observed $I(\text{LC})$ for P23, P28A, and P42 the above value of $I(\text{LC})$ seems to be typical for the central part of the quiescent prominences. Figure 5 gives the results as a function of N_e for a possible range of N_e , $10^{10} \leq N_e \leq 10^{11.4}$, in the central part of the quiescent prominences (Hirayama, 1979). In the calculations we have assumed $N_e = N_p$. It should be noted again that the uncertainty of the results in Figure 5 is less than 30% for the temperature range of $4500 \leq 8500$ K.

Figure 5 shows that $N_p/N_{\text{HI}} \leq 1.9$ in the central of the model prominence. For $N_e \geq 2 \times 10^{10}$ the degree of ionization of hydrogen corresponds to the value $N_p/N_{\text{HI}} < 1$ which is less than that inferred from observations of the visual spectrum and from most theoretical calculations (e.g., Tandberg-Hanssen, 1974; Hirayama, 1979). Therefore, we cannot estimate the total density from N_e in the central part of the prominences. For $N_e \geq 3 \times 10^{10}$, $N_{\text{HI}} + N_p$ and N_{HI} are a factor of 2 or more larger than N_e . This low degree of ionization may suggest that the LC radiation from the chromosphere and the corona is not completely penetrating into the central part of the prominences. From the results of Figure 5 it is found that the column density of hydrogen corresponding to $\tau_{\text{H}} = 50$ ranges $8.5 \times 10^{18} \leq (N_{\text{HI}} + N_p) d \leq 2.3 \times 10^{19} \text{ cm}^{-2}$ for the model prominence, where d is the effective thickness of the prominence.

It should be mentioned here that the degree of ionization of hydrogen in Figure 5 gives a smaller value of the emission measure than the average obtained from observations of the high Balmer lines. Landman and Mongillo (1979) observed the high Balmer lines ($i = 10-22$) in seven quiescent prominences. Their results showed

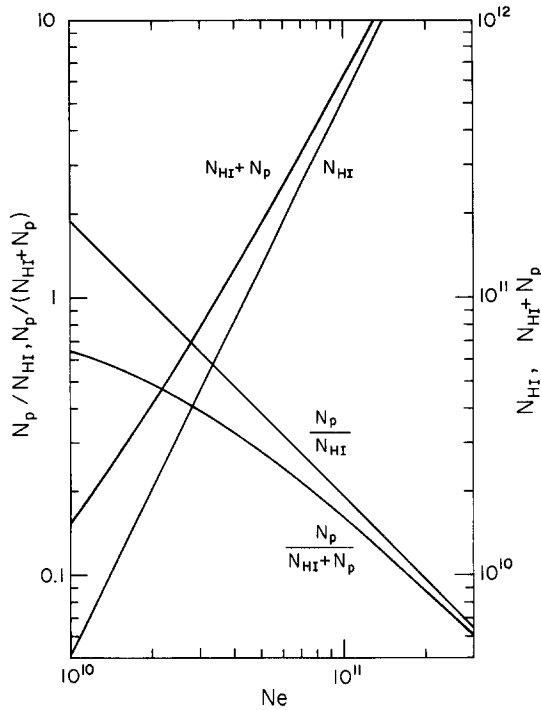


Fig. 5. Degree of ionization of hydrogen and the total and neutral hydrogen density as a function of N_e for the central part of a model prominence with $T = 6600$ K and $I(\text{LC}) = 20 \text{ erg cm}^{-2} \text{ s}^{-1} \text{ sr}^{-1} \text{ \AA}^{-1}$. These quantities are rather insensitive to T (see text).

that the limit of $(2i^2)^{-1} N_i d$ for $i \rightarrow \infty$ is $\approx 1.9 \times 10^8 \text{ cm}^{-2}$ on the average, where N_i is the population of the level with the principal quantum number i of hydrogen. This value corresponds to $N_e N_p T^{3/2} d \approx 9.1 \times 10^{23}$. On the other hand, Equation (14) gives $N_e N_p T^{-3/2} d = 2.8 \times 10^{23}$ for $\tau_H = 50$ and $I(\text{LC}) = 20 \text{ erg cm}^{-2} \text{ s}^{-1} \text{ sr}^{-1} \text{ \AA}^{-1}$, assuming $T = 6600$ K. This discrepancy may be explained by assuming that the degree of ionization of hydrogen increases outside the central part of the prominences.

The means that either the temperature or the source function of the LC, or both increase with height in the prominences. Therefore, the assumption of a constant $S_{\lambda c}$ in Equation (7) may not be valid outside the central part of the prominences. Since the present analysis has relied on $I(\text{LC})$ data at positions in the prominences with $\tau_H \geq 2.46$, the results should not seriously suffer from the invalidity of the assumption of a constant $S_{\lambda c}$ outside the central part of the prominences.

4. Conclusions

The two-dimensional determination of τ_H in the three prominences observed above the limb shows that the value of τ_H varies over a wide range at positions even in a single prominence. At the central part of the prominences where the opacity is

largest τ_H reaches a maximum value of 30 to 50 for the three prominences. In general τ_H decreases with height in the prominences. Most positions near the outer boundary of the prominences are optically thin in the LC ($\tau_H < 1$). It is found that the determination of τ_H for P23 is consistent with the data of the Mg x spectroheliogram.

The calculations of the degree of ionization for a model prominence show that hydrogen is less than half ionized for $N_e \geq 2 \times 10^{10}$ in the central part of the prominence. This may suggest that the LC radiation from the chromosphere and the corona does not completely penetrate into the central part of the prominence. The emission measure derived from observations of the high Balmer lines may be explained by assuming that the degree of ionization of hydrogen increases outside the central part of the prominence.

Acknowledgements

One of the authors (M.K.) is grateful for the opportunity of visiting the Center for Astrophysics under the auspices of the SAO Langley-Abbot Program for Solar Research. This work was also supported in part by NASA contract 5-3949.

References

- Dupree, A. K. and Reeves, E. M.: 1971, *Astrophys. J.* **165**, 599.
 Feldman, U. and Doschek, G.: 1977, *Astrophys. J. Letters* **216**, L119.
 Heasley, J. N. and Mihalas, D.: 1976, *Astrophys. J.* **205**, 273.
 Heasley, J. N. and Milkey, R. W.: 1976, *Astrophys. J.* **210**, 827.
 Heasley, J. N. and Milkey, R. W.: 1978, *Astrophys. J.* **221**, 677.
 Hirayama, T.: 1963, *Publ. Astron. Soc. Japan* **15**, 122.
 Hirayama, T.: 1964, *Publ. Astron. Soc. Japan* **16**, 104.
 Hirayama, T.: 1979, in E. Jensen, P. Maltby, and F. Q. Orrall (eds.), 'Physics of Solar Prominences', *IAU Colloq.* **44**, 4.
 Kanno, M.: 1979, *Publ. Astron. Soc. Japan* **31**, 115.
 Kjeldseth Moe, O., Cook, J. W., and Mango, S. A.: 1979, *Solar Phys.* **61**, 319.
 Landman, D. A. and Mongillo, M.: 1979, *Solar Phys.* **63**, 87.
 Noyes, R. W. and Kalkofen, W.: 1970, *Solar Phys.* **15**, 120.
 Noyes, R. W., Dupree, A. K., Huber, M. C. E., Parkinson, W. H., Reeves, E. M., and Withbroe, G. L.: 1972, *Astrophys. J.* **178**, 515.
 Orrall, F. Q. and Schmahl, E. J.: 1976, *Solar Phys.* **50**, 365.
 Poland, A., Skumanich, A., Athay, R. G., and Tandberg-Hanssen, E.: 1971, *Solar Phys.* **18**, 391.
 Reeves, E. M., Timothy, J. G., and Huber, M. C. E.: 1974, *Proc. S.P.I.E.* **44**, 159.
 Reeves, E. M., Huber, M. C. E., and Timothy, J. G.: 1977a, *Appl. Opt.* **16**, 837.
 Reeves, E. M., Timothy, J. G., Huber, M. C. E., and Withbroe, G. L.: 1977b, *Appl. Opt.* **16**, 849.
 Schmahl, E. J. and Orrall, F. Q.: 1979, *Astrophys. J. Letters* **231**, L41.
 Schmahl, E. J., Foukal, P. V., Huber, M. C. E., Noyes, R. W., Reeves, E. M., Timothy, J. G., Vernazza, J. E., and Withbroe, G. L.: 1974, *Solar Phys.* **39**, 337.
 Tandberg-Hanssen, E.: 1974, *Solar Prominences*, D. Reidel Publ. Co., Dordrecht, Holland.
 Vernazza, J. E. and Noyes, R. W.: 1972, *Solar Phys.* **22**, 358.
 Vernazza, J. E. and Reeves, E. M.: 1978, *Astrophys. J. Suppl.* **37**, 485.
 Withbroe, G. L.: 1970, *Solar Phys.* **11**, 208.